Multicolor photoluminescence from non-conjugated poly(3,4-dihydropyran) nanoparticles

Lorenzo Vallan, Anh Thy Bui, Gediminas Jonusauskas, Nathan Mcclenaghan, Emin Istif, Daniele Mantione, Eleni Pavlopoulou, Cyril Brochon, Georges Hadziioannou, Eric Cloutet

Multicolor photoluminescence from non-conjugated poly(3,4-dihydropyran) nanoparticles

Lorenzo Vallan,[a] Anh Thy Bui,[b]* Gediminas Jonusauskas,[c] Nathan D. McClenaghan,[b] Emin Istif,[a] Daniele Mantione,[a] Eleni Pavlopoulou,[a,d] Cyril Brochon,[a] Georges Hadziioannou,[a] Eric Cloutet*[a]*

[a.] Laboratoire de Chimie des Polymères Organiques (LCPO-UMR 5629), Université de Bordeaux, Bordeaux INP, CNRS, F-33607 Pessac, France.

[b.] Institut des Sciences Moléculaires UMR 5255 CNRS/Université de Bordeaux 351, Cours de la Libération 33405 Talence Cedex, France.

[c.] Laboratoire Ondes et Matière d'Aquitaine UMR 5798, CNRS/Université de Bordeaux 351, Cours de la Libération 33405 Talence Cedex, France.

[d.] Institute of Electronic Structure and Laser, Foundation for Research and Technology—Hellas, 71110 Heraklion Crete, Greece

ABSTRACT In recent years, non-conjugated organic luminophores are receiving considerable interest from the scientific community, offering new conceptual basis for the development of alternative photoluminescence-based technologies. In this work, the polymerization of 3,4-dihydropyran was exploited for the preparation of non-conjugated photoluminescent polymer nanoparticles. Remarkably, excitation-dependent multicolor emission ranging from blue to yellow

was observed both in solid and in solution. In contrast with similar materials, this behavior was not attributed to aggregation-induced emission, but rather to the presence of independent, non-interacting chromophores located on the polymer structure. Structural and optical characterization along with further chemical modifications suggest that the emission is related to the presence of acetal groups formed by ring-opening polymerization. In addition, it was shown that the removal of unsaturated structures could enhance the photoluminescence quantum yield of the polymer (QY) up to 0.20 (λ_{ex} = 355 nm). This work provides a new type of non-conjugated organic luminophore with both high QY and multicolor emission.

Introduction

Luminescence, resulting from the relaxation of an excited state to a ground state via the emission of a photon, nowadays finds widespread uses for the most disparate applications in the chemistry, biology and medicine fields. While the most common and studied class of luminescent materials are undoubtedly planar organic molecules with extended π-conjugated structures, many other types of luminescent materials are based on organic aromatic polymers,[1] rare earth-based organic complexes,[2] fluorescent proteins,[3] semiconductor nanoparticles[4] and carbon nanomaterials with extended aromatic domains.[5,6] A common feature for the aforementioned emitters is that the chemical structures, as well as the electronic transitions involved, are well-understood. With respect to purely organic luminophores, structure planarity, electron delocalization and unoccupied p-orbitals are considered essential features for the observation of luminescence. Nonetheless, in 2001, in their work on PAMAM (poly(amidoamine)) blue fluorescence, Larson and Tucker proposed the existence of non-traditional intrinsic luminophores (NTIL), i.e., organic compounds displaying emission in absence of aromatic structures.[7] While the exact mechanism behind this

phenomenon is not yet understood, it was proposed that the clustering of electron-rich groups enables a through-space conjugation via n–π* transitions, which is at the origin of this type of non-traditional luminescence.[8] The immobilization of the electron-rich groups into rigid structures is an effective way to promote the radiative relaxation over the non-radiative one and can be achieved by different strategies, such as molecules aggregation, covalent crosslinking or substrate immobilization.[9] Lately, in conjunction with the emergence of new classes of nanostructures, such as carbon dots (CDs)[10] and carbon polymer dots (CPDs),[11,12] the interest in NTIL has increased enormously, as these materials are highly fluorescent and present many potential advantages over traditional dyes, especially in terms of photostability, cost and ease of production. Therefore, the identification of new NTIL as an alternative to conventional dyes is extremely desirable and several types of polymeric NTIL have been discovered. Those containing amide groups are probably the most widespread;[10,11,13–19] in fact amide is able to provide rigidity to the structure, thanks to both the partial sp^2 character of the C-N bond and the ability to form strong H-bonds, and, in specific conditions of rigidity, it can act as chromophore and emissive center.[20] Additionally, other types of NTIL have been studied, including polyanhydride,[21,22] poly(aminoester),[23] poly(maleic anhydride-alt-vinyl acetate),[21,24] poly(urea),[25] poly(urethane),[26] poly(nitrile),[27] poly(thioethersulfone),[28] poly(siloxane)[29] and poly(alkylborate).[30] Even in absence of a sp^2-hybridized carbon, such as in the case of poly(ethyleneimine)[31,32] and poly(ethylene glycol),[33,34] fluorescence emission was detected. Nevertheless, in the case of poly(ethylene glycol) high concentrations of material were required for the enhancement of the emission and only blue fluorescence was observed. This phenomenon has been ascribed to the clustering and rigidification of the polymer chains at high concentrations, which force oxygen groups to stay in close contact, producing the electronic clouds overlapping responsible for the emissive state.[35] In this context,

we focused our attention on dihydropyran polymer nanoparticles and report studies of their optical properties, as well as their synthesis and characterization.

In terms of synthesis, cationic polymerization of cyclic vinyl ethers has been explored in the past.[36] In particular, the monomers 2,3-dihydrofuran (DHF) and 3,4-dihydro-2*H*-pyran (DHP) can polymerize in presence of a Lewis acid via double bond opening.[37–41] Although this is the only reaction mechanism resulting in polymerization of DHF, other side reactions can also take place for DHP. As a result, DHP gives polymers that are shorter than DHF and with more heterogeneous structures. A detailed study regarding the polymerization of DHP was published by Kamio et al. in 1966, where the poly(dihydropyran) infrared spectrum revealed the presence of carbon-carbon double bonds and aldehyde groups in the polymer structure.[42] Therefore, it was concluded that, besides propagation via double bond, the DHP polymerization could also proceed via ring-opening reactions. With the aid of NMR spectroscopy, more recent studies supported those conclusions, although without providing a deeper structural analysis of the polymer.[43]

Interestingly, the polymeric nanoparticles synthesized and studied in the current work were found to be intrinsically photoluminescent both in solid and dilute solutions. Moreover, they display excitation-dependent multicolor emission ranging from blue to yellow. The relationship between these features and the chemical structure was further explored by means of physical characterization methods and chemical modification.

Results and Discussion

Synthesis, size and structure of PolyDHP. The polymerization of DHP was carried out at room temperature using $AlCl_3$ as initiator and dichloromethane as solvent. The reaction does not

require inert or anhydrous conditions and the work-up is simple. By increasing the amount of initiator, the reaction is accelerated, but no changes in the polymer size or in the structure were observed (Figure S1, Figure S2 and Table S1). Other acid initiators were also tested, such as *p*-toluenesulfonic acid and trifluoroborane etherate, and polymeric products with comparable structures were obtained (Figure S3). The mass of PolyDHP was estimated by size-exclusion chromatography, obtaining a Mn of 9.8×10^2 with a dispersity (Đ) value of 1.7. This result was confirmed by MALDI mass spectrometry, which detected the presence of polymer chains with mass-to-charge ratios comprised between 779.52 and 1049.71 Da/e (Figure S4). The low molecular weight found is comparable to the values reported in previous studies[39,40] and corresponds to chains with an average length of about 10 repeat units. The height of the polymer nanoparticles was measured by AFM (Figure 1). The height profile reveals that the polymer consists of nanoparticles with an average size of 2-3 nm. DOSY analysis of polymer solutions ranging from 2 to 20 mg/ml were also performed (Figure S5). The hydrodynamic radius calculated for the less concentrated sample is 2.5 nm and it increases by increasing the concentration, suggesting that aggregation takes place in solution. Notably, no signal of smaller organic compounds was detected by DOSY.

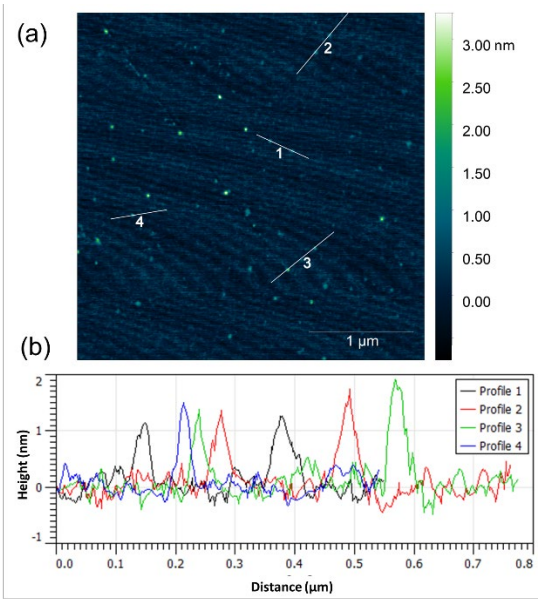

Figure 1. (a) AFM picture and (b) profiles of PolyDHP.

Structural elucidation of PolyDHP was achieved by means of infrared spectroscopy (IR), nuclear magnetic resonance spectroscopy (NMR) and X-ray photoelectron spectroscopy (XPS). In the infrared spectrum (Figure 2b), the vibrational modes related to aliphatic ethers can be recognized. The bands at 2937 and 2850 cm^{-1} correspond to the C-H stretching of bonds involving carbons that are, respectively, not bonded and bonded to oxygen atoms. The vibrational bands centered at 1450 cm^{-1} correspond to the C-H bending. C-O-C stretching produces multiple bands at 1080 and 1023 cm^{-1} (asymmetric mode) and 911 and 867 cm^{-1} (symmetric mode), whose positions are characteristic of cyclic ethers. Finally, the small bands centered at 1689 cm^{-1} could be related to sp^2 carbon, possibly belonging to traces of single alkenes on the polymer structure. ^{1}H NMR, APT and HSQC NMR spectra of PolyDHP (Figures 2c, 2d and 2e) reveal the presence of two different structures composing the polymer chain. In the ^{1}H NMR spectrum, the signals between 2.5 and 1.0 ppm correspond to hydrogens bonded to aliphatic carbons without oxygen neighbors, while the signals between 4.0 and 3.0 ppm are

relative to hydrogens bonded to carbons with oxygen neighbors. Both these groups of signals are supporting the presence of the repeat unit A (Scheme 1), which is the expected product of the polymerization via double bond opening. Nevertheless, if the entire polymer consisted only of this structure, the ratio between the intensities of the two sets of proton signals would be of 5:3, while in the recorded spectrum it is closer to 2:1. Furthermore, a third type of signal, not attributable to the repeat unit A, is found at 4.5 ppm in the ^{1}H spectrum and at 99 ppm in the APT spectrum and it unambiguously reveals the presence of the acetal group. Acetal formation can only be explained by the occurrence of a ring opening reaction, where the DHP oxygen acts as nucleophile towards a living carbocation and the resulting oxonium cation is neutralized by further cleavage of the DHP C-O bond. Interestingly, through this mechanism a carbon-carbon double bond is introduced in the polymer skeleton and its involvement in further polymerization would produce a branching point, depicted in Scheme 1 as repeat unit B. As a first approximation the entire polymer can be described as comprising two repeat units, indicated in Scheme 1 as A and B, generated respectively by double bond addition and a ring-opening reaction. Starting from this assumption, an estimation of the ratio between repeat unit A and repeat unit B was attempted. Knowing from the ^{1}H signals integration (Figure 2C) that the proportion between the three types of protons is 41:19:1, and that the number of acetal's protons corresponds the number of repeat units B, an A/B ratio between 5 and 6 was calculated (see page S12 of Supporting Information for details). However, it should be noted that this value is based on the hypothesis that no other structure is present on the polymer, which is not completely accurate.

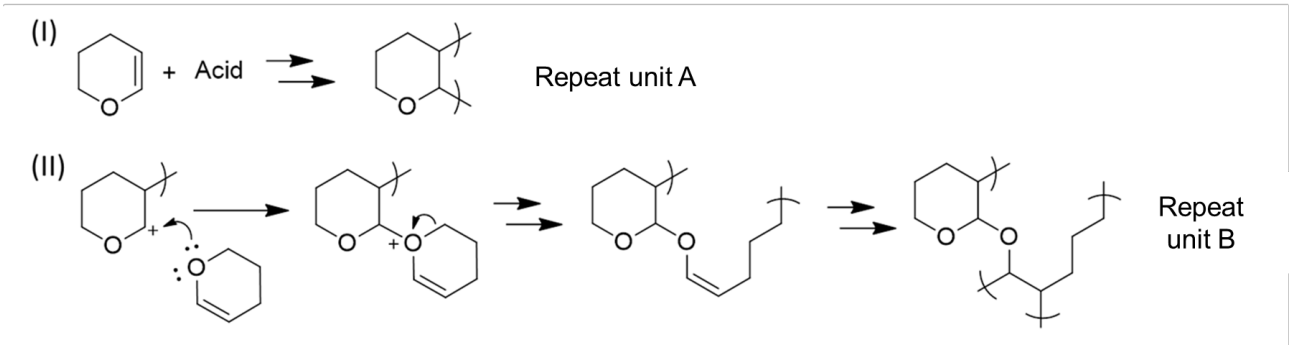

Scheme 1. (I) Double bond opening and (II) ring opening polymerization of DHP. The catalytic role of $AlCl_3$ is omitted for clarity.

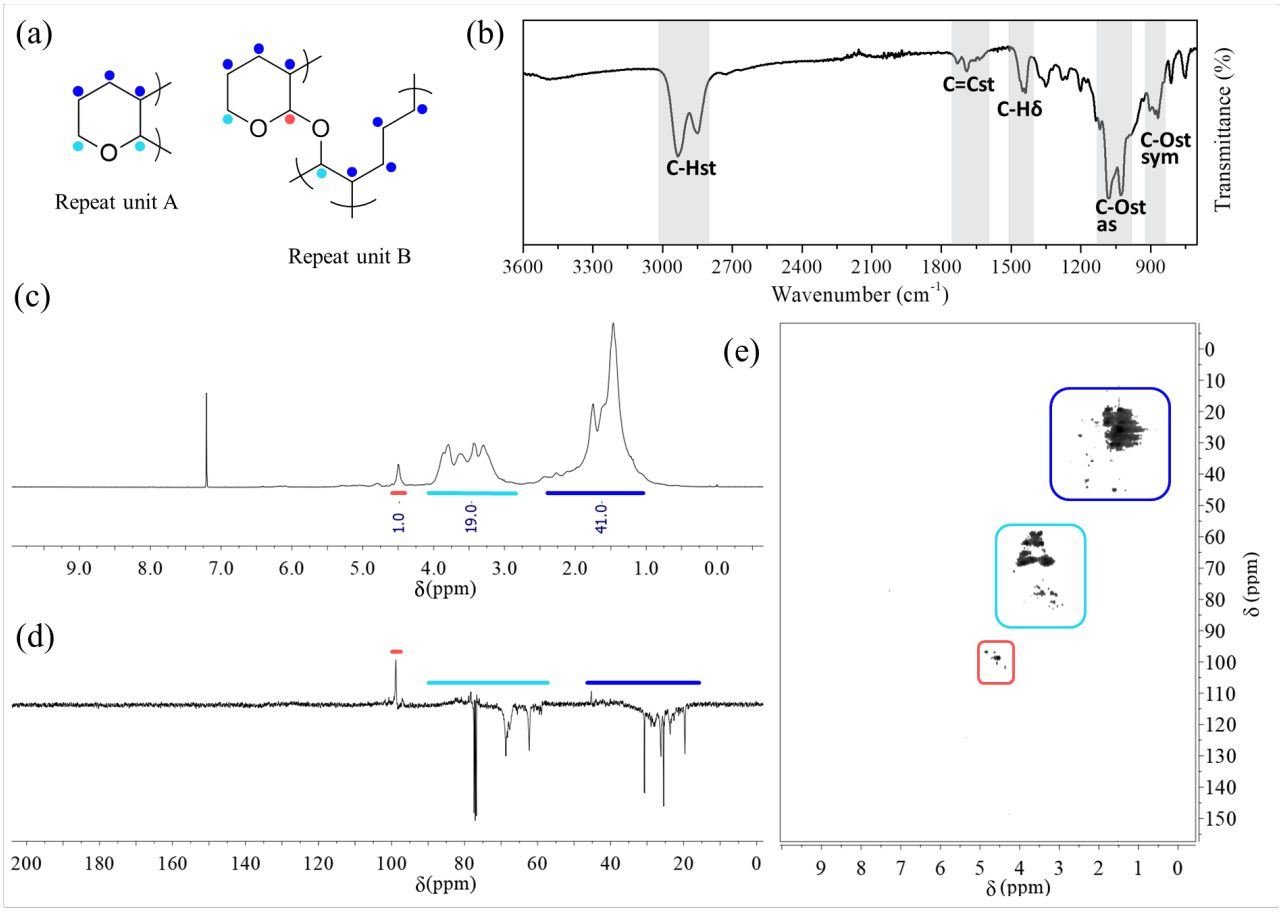

Figure 2. (a) Repeat units of PolyDHP with color assignment, (b) infrared spectrum, (c) ^{1}H NMR spectrum in $CDCl_3$, (d) APT NMR spectrum in $CDCl_3$ and (e) HSQC spectrum of PolyDHP in $CDCl_3$.

In fact, the very weak signals observed between 5.3 and 4.8 ppm in the proton spectrum could belong to traces of the alkene precursors of the repeat unit B, as well as the stretching band at 1689 cm^{-1} in the IR spectrum. The characterization by XPS spectroscopy confirmed the polymer structure inferred by NMR and IR. It can be noticed from the XPS survey (Figure 3a) that the sample consists purely of carbon and oxygen elements. Chlorine is present only in traces and the absence of aluminum proves the effectiveness of the work-up procedure (Figure S7). The quantitative elemental analysis (Table S2) reveals that the DHP carbon/oxygen ratio of 5 to 1 is preserved in polyDHP, thus excluding addition or elimination of water or other molecules during the polymer formation. The C1s peak deconvolution (Figure 3b, Table S3) produces four components, corresponding to: a) carbon bonded to carbon only (284.46 eV); b) tertiary carbon bonded to oxygen (285.25 eV); c) secondary carbon bonded to oxygen (286.00 eV); d) acetal carbon (287.40 eV). The O1s deconvolution (Figure 3c, Table S3) reveals only two types of oxygen: an ether oxygen at 532.36 eV and an acetal oxygen at 533.30 eV. All together, these data are in agreement with the copolymer structure formed by the repeat units A and B of Scheme 1.

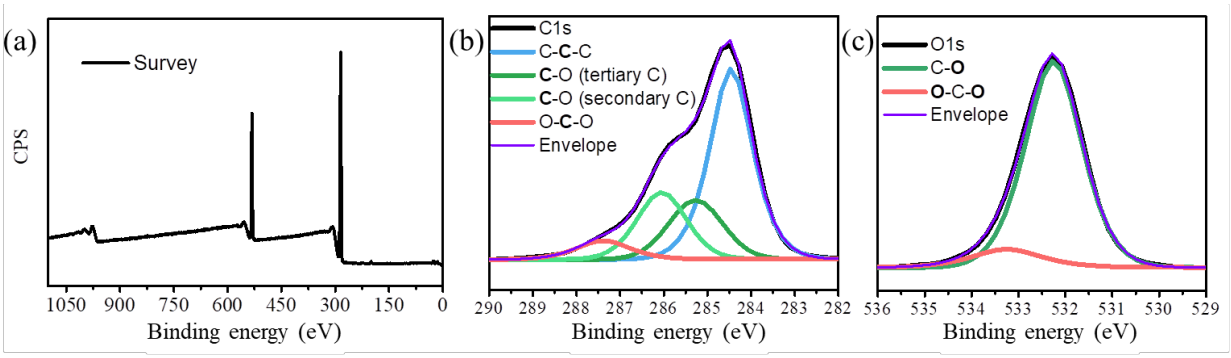

Figure 3. (a) XPS survey, (b) C1s and (c) O1s of PolyDHP.

Optical properties. PolyDHP optical properties were studied by electronic absorption, steady-state and time-resolved photoluminescence spectroscopy. The nanoparticles are photoluminescent both in solution and powder form (Figure 4a and Figure S8). In the absorption spectrum of PolyDHP in THF, a broad absorption window is observed extending from the UV spectral region to over 500 nm (Figure S9), while the photoluminescence excitation spectrum shows a clearly defined band, which is attributed to an electronic transition upon photoexcitation that gives rise to the observed luminescence. A moderate apparent shift is observed between the excitation and emission band maxima, for example, the photoluminescence emission maximum is at 445 nm when the excitation band maximum is at 360 nm. Furthermore, the wavelength maximum of the observed emission was found to be dependent on the excitation wavelength, which would not be anticipated if a single emissive state were present. Figures 4b and c show normalized excitation and emission spectra obtained upon detecting and exciting at various wavelengths (for full map see SI, Figure S10). A shift between maxima of excitation and emission band, between 60 – 110 nm ($\Delta\bar{\nu}$ = 4000 – 7500 cm^{-1}) depending on the excitation wavelength, is observed. Consequently, emission wavelength tuning can be achieved in the blue

to yellow region on varying excitation wavelength, as illustrated through the CIE color space diagram in Figure 4d.

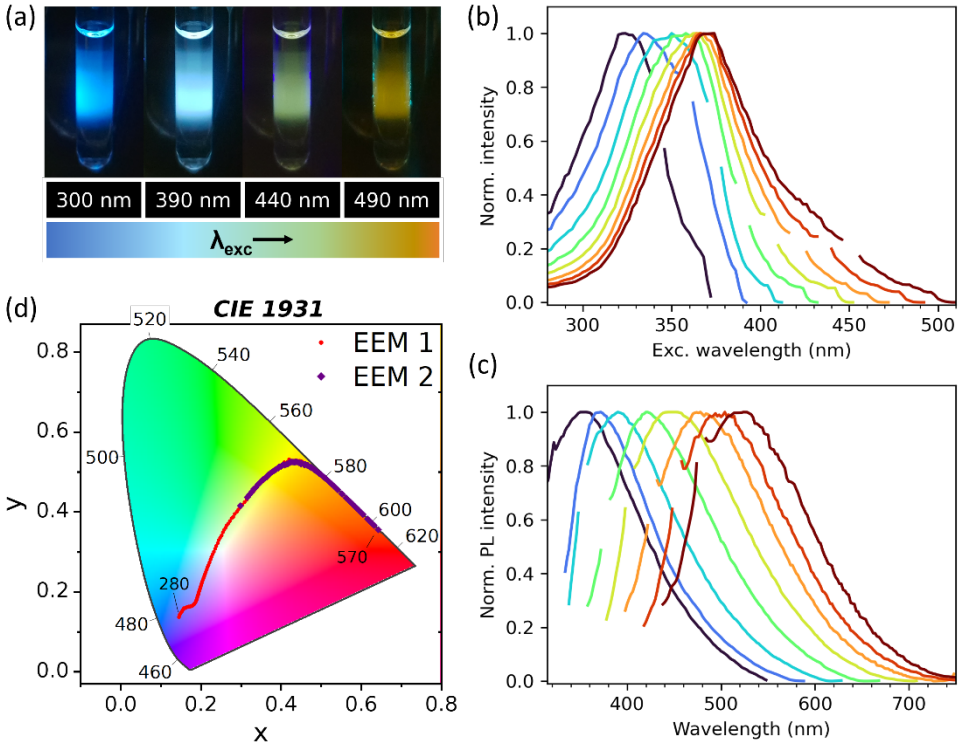

Figure 4. Excitation wavelength-dependent photoluminescence of an optically dilute solution of PolyDHP in THF. a) Photographs of a solution of PolyDHP in THF at different excitation wavelengths; b) Normalized excitation spectra at different detection wavelengths, from 380 to 520 nm, in 20 nm increments (0.1 mg/ml); c) Normalized photoluminescence spectra at different excitation wavelengths from 280 to 420 nm, in 20 nm increments (0.1 mg/ml); d) Evolution of the emission color of PolyDHP with the excitation wavelength as visualized in the CIE color space. (Excitation ranges: EEM1 = λ_{ex} = 290 – 470 nm; EEM2 = 370 – 550 nm at twofold higher concentration).

Photoluminescence intensity was found to be linearly proportional to concentration under 0.64 mg/ml, suggesting the absence of aggregation-induced emission in this concentration range (Figure S11). In order to gain further insights into the nature of the emitting state, time-resolved spectroscopy was performed at varying temperatures in THF and at room temperature in hexanol, a solvent showing relatively slow solvent reorganization dynamics. Figure 5a shows the evolution of the emission of a reference coumarin-481 (C481) dye on the sub-nanosecond timescale.[44] The solvent retards reorganization and relaxation of the excited molecule, accompanying a changing dipole and/or geometry, and as a result a red shifting of emission during the lifetime of the excited state is clearly seen. In contrast, the polymer emitter shows essentially no spectral shifting neither in hexanol (Figure 5b) nor in THF (Figure 5c). From this result we can tentatively suggest that for the emissive polymer: a) there is no major charge or structural reorganization between ground and excited state of the emitting species; b) efficient electronic energy transfer does not occur between polymer chromophores following excitation. Indeed, this observation is consistent with the presence of multiple, independent and orthogonal chromophores suggested by the observation of the excitation wavelength dependence on emission.

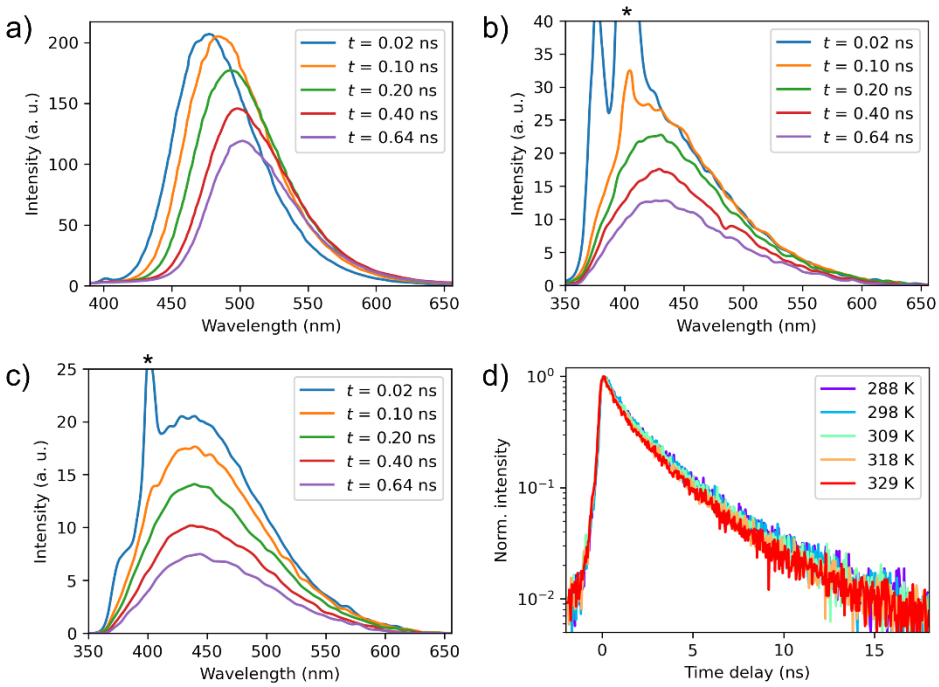

Figure 5. a) Photoluminescence emission of C481 in hexanol at different times (t) post-excitation (λ_{ex} = 355 nm); b) Photoluminescence emission of PolyDHP in hexanol at different times (t) post-excitation (λ_{ex} = 355 nm); c) photoluminescence emission of PolyDHP in THF at different times (t) post-excitation at room temperature (λ_{ex} = 355 nm); d) Photoluminescence decays of PolyDHP at varying temperature in the range 278 – 330 K in THF (λ_{ex} = 355 nm) measured in spectral region 425 – 475 nm. Asterisks indicate Raman scattering signals.

It is widely known that in some cases the aggregation of NTIL can greatly affect their emission intensity.[22,29,45–47] If the emitting species is effectively a supramolecular aggregate, varying temperature may be anticipated to affect the structural organization and rigidity and consequently the emission. For a given chromophore, the photoluminescence quantum yield is inversely proportional to the radiative decay rate and hence proportional to the luminescence lifetime. Thus, luminescence lifetime can be considered a powerful tool to probe changes of an emissive state, devoid of artifacts linked to emission intensity measurements over a range of temperatures

such as, for example, changing refractive index or light scattering. As shown in Figure 5d, relatively short (circa 1.5 ns) emission decays at varying temperatures in the range 278 – 330 K in THF follow a non-exponential decay and show only very small variations with temperature in this range. Equally, the emissive species were found to give unchanging emission in aprotic THF, DMF and protic ethanol, with a slight red-shift in chloroform (Figure S12). Therefore, PolyDHP photoluminescent behavior does not rely on weak intermolecular interactions forming supramolecular aggregates and it should be rather ascribed to the individual polymer nanoparticles. Recently, several works reported the existence of NTILs displaying phosphorescence in solid state.[48,49] In here, PolyDHP solid power and a frozen THF solution (77 K) were characterized by time-resolved spectroscopy, but no long component could be detected and the characteristics times remain consistent with combinations of numerous fluorescence signals (Figure S13).

Investigation on the chemical structures responsible for photoluminescence emission. Determination of whether the observed photoluminescence emission is intrinsically related to the described polymer structure, rather than a more classical description of an organic fluorophore, is crucial for further understanding of the phenomenon. In principle, traces of a highly emissive conjugated dye could be present below the detection limit of NMR spectroscopy and still be responsible for the photoluminescence emission. In this scenario, it would be anticipated that the dye would exist and emit also in the unbounded form, i.e. not attached to the polymer structure. Column chromatography on silica gel was performed to eliminate any unbound dye using an elution gradient, from pure ethyl acetate to ethyl acetate/methanol (9:1, v/v). In fact, despite the low polarity of the repeat unit, PolyDHP nanoparticles have high affinity for the stationary phase because of the large number of intermolecular interactions between polymer and silica, and they

can be displaced only by a highly polar eluent. Instead, a hypothetical low-molecular weight dye is expected to have higher affinity for the mobile phase even at lower polarity. Nevertheless, only a single photoluminescent product was collected from the column and, by SEC and NMR analysis (Figure S14 and S15), it was found to correspond to the polymer whose structure and size were previously described, excluding the possibility of a molecular dye as the origin of the photoluminescence emission. Equally, emission wavelength dependent on excitation wavelength is not a behavior associated with small molecule emitters.

In order to get more hints about the chemical structures originating the photoluminescence emission of PolyDHP, a comparison with poly(2,3-dihydrofuran) (PolyDHF) was made. 2,3-dihydrofuran (DHF) was polymerized in the same way as for DHP and after purification a solid white powder was obtained. The structure was confirmed by ^{1}H and ^{13}C NMR (Figure S16). From these spectra it is clear that the polymerization of DHF proceeds exclusively via double bond opening, as already ascertained in previous studies.[40] The photoluminescence emission maximum of PolyDHF was found at 420 nm for λ_{exc} = 350 nm. Nevertheless, the emission of PolyDHF is negligible (Figure S17), suggesting that the photoluminescent structures are formed from reactions occurring during PolyDHP polymerization but not during PolyDHF polymerization. As ascertained by the previous structure characterization, the polymerization of PolyDHP proceeds not only by double bond opening but also by ring opening, which is reflected in the presence of acetal groups. Therefore, the influence of this moiety on the photoluminescence emission was investigated. PolyDHP was dissolved in methanol/dichloromethane, 1:1 (v/v) and an excess of *p*-toluenesulfonic acid was added. Subsequently, the acid was removed and PolyDHP was isolated and characterized. This procedure allowed the cleavage of acetal groups, as shown by the absence of the characteristic

resonance attributed to an acetal in the ^{1}H NMR spectrum of PolyDHP after the treatment (Figure S18). Interestingly, acetal cleavage resulted in a drastic reduction of the photoluminescent emission of the polymer (Figure S19). In fact, the apparent PLQY of PolyDHP at λ_{exc} = 350 nm passed from 0.07 before cleavage to 0.01 after cleavage. Therefore, this could be consistent with a determinant role of acetals' branching points in the achievement of constrained polymer conformations, where several oxygen atoms, including acetal's oxygens, are brought in forced proximity one to each other. As previously reported, the entangled environment could promote a partial through space-conjugation between oxygens' lone pairs, providing new available excited states from where the radiative relaxation occurs.[27,50,51] Also, it could be hypothesized that various cyclic and macrocyclic configurations locked by acetal groups are originated during the polymerization (i.e. by intramolecular polymerization reactions), which could further increase structural rigidity. In this scenario, acetal cleavage would provide more conformational freedom to the polymer and decrease oxygens density.

It was reported that besides acetal groups, the ring opening polymerization mechanism can produce unsaturated side products, i.e., alkenes and carbonyls (Figure S20).[42] As observed from NMR and IR characterization, their presence was found to be minimal in the PolyDHP structure. Nevertheless, any possible involvement in photoluminescence emission should be investigated. Chemical treatment of PolyDHP by mixing with an excess of borane-THF complex was performed, borane being known to react with several types of unsaturated groups. Later, a NaOH solution was added. After purification and isolation, the resulting material appeared as a pale-yellow solid powder. Size and molecular weight of the borane-treated PolyDHP (btPolyDHP) were characterized respectively by AFM and SEC, revealing no changes with respect to PolyDHP (Figure S21 and S22). Structural characterization was also performed. ^{11}B NMR

spectroscopy ascertained the absence of boron after the work up (Figure S23). ^{1}H NMR analysis showed that acetal groups were not affected by the borane treatment (Figure S24). On the contrary, in the infrared spectrum the weak bands related to alkene stretching modes are no longer present, confirming that the alkene and/or carbonyl groups reacted with borane (Figure S25). The removal of unsaturations is reflected in the paler color of the solid (see Figure 6).

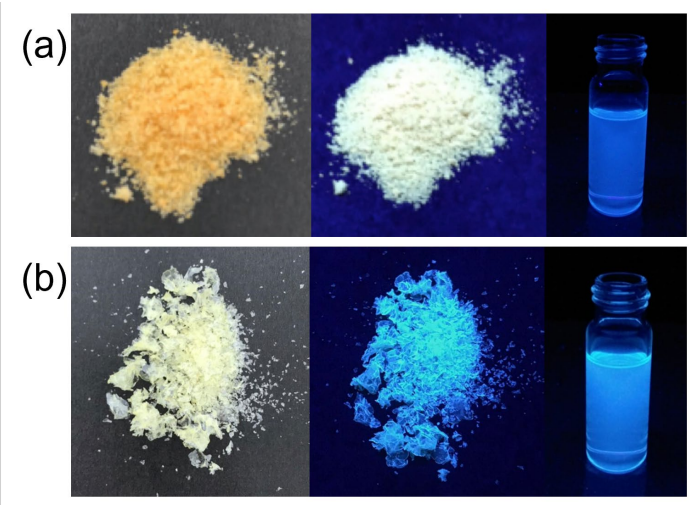

Figure 6. (a) PolyDHP in powder under visible (top-left) and UV light (top-middle) and in THF solution (1 mg/ml) under UV light (top-right), (b) btPolyDHP in powder under visible (bottom-left) and UV light (bottom-middle) and in THF solution (1 mg/ml) under UV light (bottom-right).

Equally, the emission properties of the polymer are greatly affected (Figure S26). Figure 7 shows the excitation-dependent photoluminescence (PL) quantum yield of the polymer before and after borane treatment, obtained from a recomposed excitation-emission map (EEM) (Figure S27). As previously done in the analysis of PolyDHP (Figure 4), optically dilute solutions of two different concentrations of btPolyDHP were used (resulting in two maps EEM1 & 2), the latter being two times more concentrated to compensate for the extremely low absorption in the visible region. The plot was calibrated by a quantum yield value determined by relative method (Figure

S28). The similarity of values obtained in the shared spectral region (380 - 470 nm) attests to the validity of this approach. A net, circa 2-3-fold increase, in emission is observed across the whole emission spectral region, following the borane treatment. It was further noted that while the maximal quantum yield was achieved at λ_{exc} = 364 nm for both PolyDHP (Φ = 0.07) and btPolyDHP (Φ = 0.20), one red-shifted population of green emitters (λ_{exc} = 440 nm; Φ = 0.12) becomes more prominent in btPolyDHP as a result of this treatment. These results rule out the direct participation of unsaturated structures to the photoluminescence emission. Moreover, the borane treatment could be responsible for further intra- and/or inter-molecular crosslinking at the expense of these structures. According to this possibility, the higher QY of btPolyDHP with respect to PolyDHP could be related to the further rigidification of the polymer chains by crosslinking, which can effectively suppress the vibrational and rotational freedom of oxygen groups and promote the radiative decay of the photoexcited state.

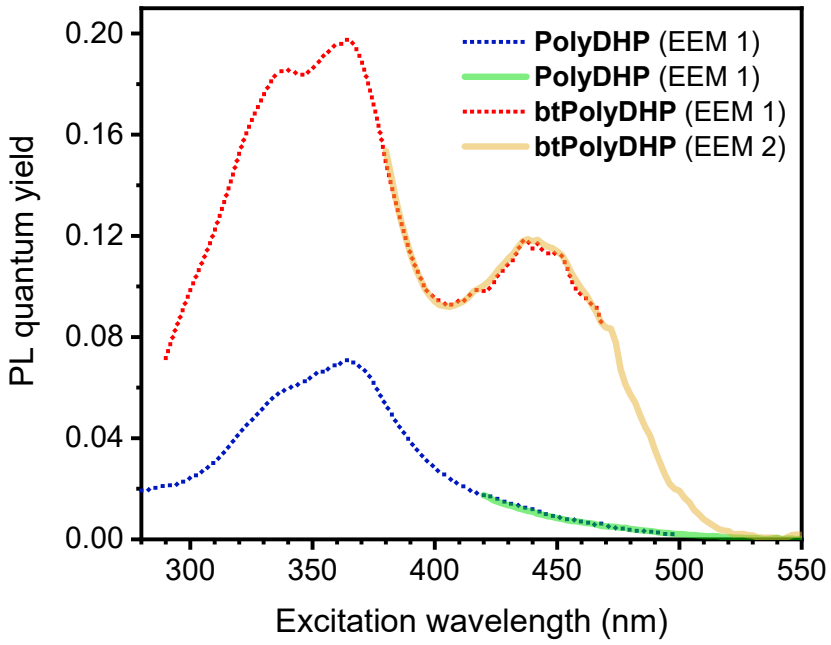

Figure 7. PL quantum yield of PolyDHP and btPolyDHP in THF as a function of the excitation wavelength. (Excitation ranges: EEM1 = λ_{ex} 290 – 470 nm; EEM2 = 380 – 550 nm at twofold higher concentration)

Conclusions

Herein we report a new addition to the emerging class of non-traditional intrinsic luminophores (NTIL), namely a luminescent non-conjugated polydihydropyran (polyDHP) polymer, consisting of nanoparticles of 2-3 nm average size. Remarkably, discrete excitation wavelength-dependent emission ranging from blue to yellow is observed even for dilute solutions. Although a solid theoretical platform for this class of compounds and description of the emitter in general warrants development, which is beyond the scope of the current work, experimental evidence gave some indications on the nature of the emitters. Optical spectroscopy measurements point to a myriad of independent, non-interacting chromophores with sub-nanosecond lifetimes, which are largely insensitive to temperature and the solvent environment, thus excluding an aggregation-dependent fluorescence mechanism. Instead, proof-of-concept experiments suggest the key-role of acetals in the peculiar emissive behavior of PolyDHP, while the presence of unsaturated side-products formed during polymerization is shown to be detrimental in terms of quantum yield. These results supply new insights to the understanding of NTIL-based materials and provide a new strategy for the simple and cheap synthesis of multicolor photoluminescent polymer nanoparticles.

ASSOCIATED CONTENT

Supporting Information. ^{1}H NMR of PolyDHP samples obtained with different $AlCl_3$ concentrations, Size-exclusion chromatogram of PolyDHP samples obtained with different $AlCl_3$

concentrations, ^{1}H NMR of PolyDHP samples obtained with different initiators, DOSY spectra of PolyDHP at different concentrations, XPS and elemental analysis of PolyDHP, Photoluminescence spectra of solid PolyDHP, Absorption and photoluminescence spectra of PolyDHP in THF, Normalized absorbance-independent excitation-emission matrix of PolyDHP in THF, PolyDHP emission in different solvents, Size-exclusion chromatogram of PolyDHP obtained from column chromatography, ^{1}H NMR of PolyDHP obtained from column chromatography, ^{1}H NMR and ^{13}C NMR of PolyDHF, Emission spectra of PolyDHP and PolyDHF in THF, ^{1}H NMR of PolyDHP before and after acetal cleavage, Absorption and emission spectra of PolyDHP before and after acetal cleavage, AFM characterization of btPolyDHP, Size-exclusion chromatogram of btPolyDHP, ^{11}B NMR spectrum of btPolyDHP, ^{1}H NMR spectra of PolyDHP and btPolyDHP, IR spectra of PolyDHP and btPolyDHP, Excitation wavelength-dependance of btPolyDHP emission, Normalized absorbance-independent excitation-emission matrix of btPolyDHP in THF, Quantum yields of PolyDHP and btPolyDHP.

AUTHOR INFORMATION

Corresponding Authors

Lorenzo Vallan - Laboratoire de Chimie des Polymères Organiques (LCPO-UMR 5629), Université de Bordeaux, Bordeaux INP, CNRS, F-33607 Pessac, France. https://orcid.org/0000-0001-5267-4849 , e-mail: lorenzo.vallan@icn2.cat

Eric Cloutet - Laboratoire de Chimie des Polymères Organiques (LCPO-UMR 5629), Université de Bordeaux, Bordeaux INP, CNRS, F-33607 Pessac, France. https://orcid.org/0000-0002-5616-2979 , e-mail: eric.cloutet@u-bordeaux.fr

Anh Thy Bui - Institut des Sciences Moléculaires UMR 5255 CNRS/Université de Bordeaux 351, Cours de la Libération 33405 Talence Cedex, France. https://orcid.org/0000-0002-3718-7652 , e-mail: anh-thy.bui@u-bordeaux.fr

Present Addresses

Lorenzo Vallan – Nanostructured Functional Materials Group, Catalan Institute of Nanoscience and Nanotechnology (ICN2), CSIC and BIST. Campus UAB, Bellaterra, Barcelona 08193, Spain.

Emin Istif – Department of Molecular Biology and Genetics, Faculty of Engineering and Natural Science, Kadir Has University, 34083 Cibali Campus Fatih, Istanbul, Turkey.

Daniele Mantione – POLYMAT University of the Basque Country UPV/EHU, 20018 Donostia-San Sebastián, Spain; IKERBASQUE, Basque Foundation for Science, 48009 Bilbao, Spain.

Author Contributions

The manuscript was written through contributions of all authors. All authors have given approval to the final version of the manuscript.

ACKNOWLEDGMENT

The European Union is acknowledged for funding this research through Horizon 2020 research and innovation program under the grant agreement No. 800926 (HyPhOE). Ministerio de Ciencia e Innovación and Agencia Estatal de Investigación (MCIN/AEI/10.13039/501100011033, Spain) and the European Union (NextGenerationEU/PRTR) are acknowledged for funding: Ayuda RYC2021-031668-I. Dr. Andrea Turcati is acknowledged for his kind help.

REFERENCES

(1) Abelha, T. F.; Dreiss, C. A.; Green, M. A.; Dailey, L. A. Conjugated Polymers as Nanoparticle Probes for Fluorescence and Photoacoustic Imaging. *J Mater Chem B* **2020**, *8* (4), 592–606. https://doi.org/10.1039/C9TB02582K.

(2) Zhong, Y.; Dai, H. A Mini-Review on Rare-Earth down-Conversion Nanoparticles for NIR-II Imaging of Biological Systems. *Nano Res* **2020**, *12* (1).

(3) Rodriguez, E. A.; Campbell, R. E.; Lin, J. Y.; Lin, M. Z.; Miyawaki, A.; Palmer, A. E.; Shu, X.; Zhang, J.; Tsien, R. Y. The Growing and Glowing Toolbox of Fluorescent and Photoactive Proteins. *Trends Biochem Sci* **2016**, *42* (2), 111–129. https://doi.org/10.1016/j.tibs.2016.09.010.

(4) Freeman, R.; Willner, I. Optical Molecular Sensing with Semiconductor Quantum Dots (QDs). *Chem Soc Rev* **2012**, *41*, 4067–4085. https://doi.org/10.1039/c2cs15357b.

(5) Lu, H.; Li, W.; Dong, H.; Wei, M. Graphene Quantum Dots for Optical Bioimaging. *Small* **2019**, *15* (36). https://doi.org/10.1002/smll.201902136.

(6) Liu, H.; Wang, X.; Nie, R.; Wang, H. Synthesis and Biomedical Applications of Graphitic Carbon Nitride Quantum Dots. *J Mater Chem B* **2019**, *7* (36), 5432–5448. https://doi.org/10.1039/C9TB01410A.

(7) Larson, C. L.; Tucker, S. A. Intrinsic Fluorescence of Carboxylate-Terminated Polyamido Amine Dendrimers. *Appl Spectrosc* **2001**, *55* (6), 679–683. https://doi.org/10.1366/0003702011952596.

(8) Tomalia, D. A.; Klajnert-Maculewicz, B.; Johnson, K. A. M.; Brinkman, H. F.; Janaszewska, A.; Hedstrand, D. M. Non-Traditional Intrinsic Luminescence: Inexplicable Blue Fluorescence Observed for Dendrimers, Macromolecules and Small Molecular Structures Lacking Traditional/Conventional Luminophores. *Prog Polym Sci* **2019**, *90*, 35–117. https://doi.org/10.1016/j.progpolymsci.2018.09.004.

(9) Tao, S.; Zhu, S.; Feng, T.; Zheng, C.; Yang, B. Crosslink-Enhanced Emission Effect on Luminescence in Polymers: Advances and Perspectives. *Angewandte Chemie - International Edition* **2020**, *59* (25), 9826–9840. https://doi.org/10.1002/anie.201916591.

(10) Zhu, S.; Meng, Q.; Wang, L.; Zhang, J.; Song, Y.; Jin, H.; Zhang, K.; Sun, H.; Wang, H.; Yang, B. Highly Photoluminescent Carbon Dots for Multicolor Patterning, Sensors and Bioimaging. *Angewandte Chemie - International Edition* **2013**, 4045–4049. https://doi.org/10.1002/ange.201300519.

(11) Tao, S.; Zhu, S.; Feng, T.; Xia, C.; Song, Y.; Yang, B. The Polymeric Characteristics and Photoluminescence Mechanism in Polymer Carbon Dots: A Review. *Mater Today Chem* **2017**, *6*, 13–25. https://doi.org/10.1016/j.mtchem.2017.09.001.

(12) Vallan, L.; Imahori, H. Citric Acid-Based Carbon Dots and Their Application in Energy Conversion. *ACS Appl Electron Mater* **2022**, *4* (9), 4231–4257.

(13) Vallan, L.; Urriolabeitia, E. P.; Benito, A. M.; Maser, W. K. A Versatile Room-Temperature Method for the Preparation of Customized Fluorescent Non-Conjugated Polymer Dots. *Polymer (Guildf)* **2019**, *177*, 97–101. https://doi.org/10.1016/j.polymer.2019.05.041.

(14) Vallan, L.; Urriolabeitia, E. P.; Ruipérez, F.; Matxain, J. M.; Canton-Vitoria, R.; Tagmatarchis, N.; Benito, A. M.; Maser, W. K. Supramolecular-Enhanced Charge Transfer

within Entangled Polyamide Chains as the Origin of the Universal Blue Fluorescence of Polymer Carbon Dots. *J Am Chem Soc* **2018**, *140* (40), 12862–12869. https://doi.org/10.1021/jacs.8b06051.

(15) Sun, Y.; Cao, W.; Li, S.; Jin, S.; Hu, K.; Hu, L.; Huang, Y.; Gao, X.; Wu, Y.; Liang, X. Ultrabright and Multicolorful Fluorescence of Amphiphilic Polyethyleneimine Polymer Dots for Efficiently Combined Imaging and Therapy. *Sci Rep* **2013**, *3* (3036). https://doi.org/10.1038/srep03036.

(16) Zhang, H.; Dong, X.; Wang, J.; Guan, R.; Cao, D.; Chen, Q. Fluorescence Emission of Polyethylenimine-Derived Polymer Dots and Its Application to Detect Copper and Hypochlorite Ions. *ACS Appl Mater Interfaces* **2019**, *11*, 32489–32499. https://doi.org/10.1021/acsami.9b09545.

(17) Yang, H.; Zhang, J.; Song, Y.; Jiang, L.; Jiang, Q.; Xue, X.; Huang, W.; Jiang, B. Copolymerize Conventional Vinyl Monomers to Degradable and Water-Soluble Copolymers with a Fluorescence Property. *Macromol Chem Phys* **2021**, *222* (1). https://doi.org/10.1002/macp.202000263.

(18) Yang, H.; Ren, Z.; Zuo, Y.; Song, Y.; Jiang, L.; Jiang, Q.; Xue, X.; Huang, W.; Wang, K.; Jiang, B. Highly Efficient Amide Michael Addition and Its Use in the Preparation of Tunable Multicolor Photoluminescent Polymers. *ACS Appl Mater Interfaces* **2020**, *12* (45), 50870–50878. https://doi.org/10.1021/acsami.0c15260.

(19) Chen, F.; Jin, Y.; Luo, J.; Wei, L.; Jiang, B.; Guo, S.; Wei, C.; Gong, Y. Poly-L-Aspartic Acid Based Nonconventional Luminescent Biomacromolecules with Efficient Emission in Dilute Solutions for Al3+ Detection. *Int J Biol Macromol* **2023**, *226*, 1387–1395. https://doi.org/10.1016/j.ijbiomac.2022.11.251.

(20) Vallan, L.; Urriolabeitia, E. P.; Ruipérez, F.; Matxain, J. M.; Canton-Vitoria, R.; Tagmatarchis, N.; Benito, A. M.; Maser, W. K. Supramolecular-Enhanced Charge Transfer within Entangled Polyamide Chains as the Origin of the Universal Blue Fluorescence of Polymer Carbon Dots. *J Am Chem Soc* **2018**, *140* (40), 12862–12869. https://doi.org/10.1021/jacs.8b06051.

(21) Zhao, E.; Lam, J. W. Y.; Meng, L.; Hong, Y.; Deng, H.; Bai, G.; Huang, X.; Hao, J.; Tang, B. Z. Poly[(Maleic Anhydride)-Alt-(Vinyl Acetate)]: A Pure Oxygenic Nonconjugated Macromolecule with Strong Light Emission and Solvatochromic Effect. *Macromolecules* **2015**, *48* (1), 64–71. https://doi.org/10.1021/ma502160w.

(22) Shang, C.; Zhao, Y.; Long, J.; Ji, Y.; Wang, H. Orange-Red and White-Emitting Nonconventional Luminescent Polymers Containing Cyclic Acid Anhydride and Lactam Groups. *J Mater Chem C Mater* **2020**, *8* (3), 1017–1024. https://doi.org/10.1039/c9tc05948b.

(23) Yuan, L.; Yan, H.; Bai, L.; Bai, T.; Zhao, Y.; Wang, L.; Feng, Y. Unprecedented Multicolor Photoluminescence from Hyperbranched Poly(Amino Ester)s. *Macromol Rapid Commun* **2019**, *40* (17). https://doi.org/10.1002/marc.201800658.

(24) Chen, X.; Hu, C.; Wang, Y.; Li, T.; Jiang, J.; Huang, J.; Wang, S.; Liu, T.; Dong, W.; Qiao, J. Improve Quantum Yield of Poly(Maleic Anhydride-Alt-Vinyl Acetate) via Good Solvents. *Macromol Rapid Commun* **2022**, 2200653. https://doi.org/10.1002/marc.202200653.

(25) Restani, R. B.; Morgado, P. I.; Ribeiro, M. P.; Correia, I. J.; Aguiar-Ricardo, A.; Bonifácio, V. D. B. Biocompatible Polyurea Dendrimers with PH-Dependent Fluorescence. *Angewandte Chemie - International Edition* **2012**, *51* (21), 5162–5165. https://doi.org/10.1002/anie.201200362.

(26) Chen X.,Liu X.,Lei J.,Xu L.a,Zhao Z.,Kausar F.,Xie X.,Zhu X.,Zhang Y., Y. W. Z. Synthesis, Clustering-Triggered Emission, Explosive Detection and Cell Imaging of Nonaromatic Polyurethanes. *Mol Syst Des Eng* **2018**, *3* (2), 364–375. https://doi.org/10.1039/C7ME00118E.

(27) Zhou, Q.; Cao, B.; Zhu, C.; Xu, S.; Gong, Y.; Yuan, W. Z.; Zhang, Y. Clustering-Triggered Emission of Nonconjugated Polyacrylonitrile. *Small* **2016**, *12* (47), 6586–6592. https://doi.org/10.1002/smll.201601545.

(28) Kausar, F.; Zhao, Z.; Yang, T.; Hou, W.; Li, Y.; Zhang, Y.; Yuan, W. Z. Michael Polyaddition Approach Towards Sulfur Enriched Nonaromatic Polymers with Fluorescence-Phosphorescence Dual Emission. *Macromol Rapid Commun* **2021**, *42* (11). https://doi.org/10.1002/marc.202100036.

(29) He, Y.; Ding, F.; Zhao, Y.; Tian, W.; Feng, W.; Yan, H. Multicolor Emission of Nonaromatic Linear Polysiloxane Based on Local Conjugation Chains. *Polym Chem* **2022**, *13*, 6534–6542. https://doi.org/10.1039/d2py01083f.

(30) Guo, L.; Yan, L.; He, Y.; Feng, W.; Zhao, Y.; Tang, B. Z.; Yan, H. Hyperbranched Polyborate: A Non-Conjugated Fluorescent Polymer with Unanticipated High Quantum Yield and Multicolor Emission. *Angewandte Chemie - International Edition* **2022**, *61* (29). https://doi.org/10.1002/anie.202204383.

(31) Toth, V.; Hermann, P.; Vegh, D.; Zelles, T.; Geczi, Z. Study of the Intrinsic Fluorescence of a Highly Branched Cationic Dendrimer, Poly(Ethyleneimine) (PEI). *Molecules* **2019**, *24* (3690).

(32) Zhu, S.; Wang, L.; Zhou, N.; Zhao, X.; Song, Y.; Maharjan, S.; Zhang, J.; Lu, L.; Wang, H.; Yang, B. The Crosslink Enhanced Emission (CEE) in Non-Conjugated Polymer Dots: From the Photoluminescence Mechanism to the Cellular Uptake Mechanism and Internalization. *Chemical Communications* **2014**, *50*, 13845–13848. https://doi.org/10.1039/c4cc05806b.

(33) Fang, R.; Zhang, C.; Kuai, Y.; Liu, X.; Zhang, C. Enhanced Fluorescence of Nano Polyethylene Glycol Derived from the Oxidation. *J Lumin* **2019**, *209* (October 2018), 404–410. https://doi.org/10.1016/j.jlumin.2019.01.067.

(34) Sun, C.; Jiang, X.; Li, B.; Li, S.; Kong, X. Z. Fluorescence Behavior and Mechanisms of Poly(Ethylene Glycol) and Their Applications in Fe3+and Cr6+Detections, Data

Encryption, and Cell Imaging. *ACS Sustain Chem Eng* **2021**, *9* (14), 5166–5178. https://doi.org/10.1021/acssuschemeng.1c00250.

(35) Wang, Y.; Bin, X.; Chen, X.; Zheng, S.; Zhang, Y.; Yuan, W. Z. Emission and Emissive Mechanism of Nonaromatic Oxygen Clusters. *Macromol Rapid Commun* **2018**, *39* (21). https://doi.org/10.1002/marc.201800528.

(36) Kanazawa, A.; Aoshima, S. Concurrent Cationic Vinyl-Addition and Ring-Opening Copolymerization of Vinyl Ethers and Oxiranes. *Polym J* **2016**, *48* (6), 679–687. https://doi.org/10.1038/pj.2016.27.

(37) Ryu, J. H.; Jeong, J. H. Development of New Dihydropyran Linker for Solid-Phase Reaction. *Arch Pharm Res* **1999**, *22* (6), 585–591. https://doi.org/10.1007/BF02975331.

(38) Tanaka, H.; Otsu, T. Cationic Polymerization Behavior of Some Vinyl Ketone Cyclodimers. *Journal of Macromolecular Science: Part A - Chemistry* **1977**, *11* (9), 1677–1683. https://doi.org/10.1080/00222337708063084.

(39) Zhu, Q. Q.; Schnabel, W. Photopolymerization of Unsaturated Cyclic Ethers. *Polymer (Guildf)* **1998**, *39* (4), 897–901. https://doi.org/10.1016/S0032-3861(97)00360-1.

(40) Yonezumi, M.; Kanaoka, S.; Aoshima, S. Living Cationic Polymerization of Dihydrofuran and Its Derivatives. *J Polym Sci A Polym Chem* **2008**, *46* (13), 4495–4504. https://doi.org/10.1002/pola.22785.

(41) Oshiro, Y.; Shirota, Y.; Mikawa, H. Synthesis of the Polymer with Polar Side Groups. I. The Syntheses and Polymerizations of 2-(2, 2-Dicyanoethylene)-2, 3-Dihydropyran, 2-2(-Cyano-2-Carboethoxyethylene)-2, 3-Dihydropyran and 2-(2, 2-Dicarboalkoxyethylene)-2, 3-Dihydropyran. *Polym J* **1972**, *3* (2), 217–225. https://doi.org/10.1295/polymj.3.217.

(42) Kamio, K.; Meyersen, K.; Schulz, R. C.; Kern, W. *Uber Die Polymerisation von 2,3-Dihydropyran*; 1966; Vol. 90.

(43) Rsch, J.; Freitas, L. L. D. L.; Stadler, R.; Chemie, M.; Strasse, S. M.; Freiburg, W.-. Polymer Bulletin 9. **1991**, *404*, 397–404.

(44) Park G.; Jong Kang T. Dynamics of Polar Solvation for the Electromic Exicited State of Coumarin 481 with Excess Vibrational Energy. *Bulletin of Korean Chemical Society* **1998**, *19* (7), 799–802.

(45) Wang, Q.; Li, B.; Cao, H.; Jiang, X.; Kong, X. Z. Aliphatic Amide Salt, a New Type of Luminogen: Characterization, Emission and Biological Applications. *Chemical Engineering Journal* **2020**, *388* (124182). https://doi.org/10.1016/j.cej.2020.124182.

(46) Saha, B.; Ruidas, B.; Mete, S.; Mukhopadhyay, C. Das; Bauri, K.; De, P. AIE-Active Non-Conjugated Poly(N-Vinylcaprolactam) as a Fluorescent Thermometer for Intracellular Temperature Imaging. *Chem Sci* **2020**, *11* (1), 141–147. https://doi.org/10.1039/c9sc04338a.

(47) Pucci, A.; Rausa, R.; Ciardelli, F. Aggregation-Induced Luminescence of Polyisobutene Succinic Anhydrides and Imides. *Macromol Chem Phys* **2008**, *209* (9), 900–906. https://doi.org/10.1002/macp.200700581.

(48) Yang, T.; Li, Y.; Zhao, Z.; Yuan, W. Z. Clustering-Triggered Phosphorescence of Nonconventional Luminophores. *Science China Chemistry*. Science Press (China) February 1, 2023, pp 367–387. https://doi.org/10.1007/s11426-022-1378-4.

(49) Zheng, S.; Zhu, T.; Wang, Y.; Yang, T.; Yuan, W. Z. Accessing Tunable Afterglows from Highly Twisted Nonaromatic Organic AIEgens via Effective Through-Space Conjugation. *Angewandte Chemie - International Edition* **2020**, *59* (25), 10018–10022. https://doi.org/10.1002/anie.202000655.

(50) Feng, Y.; Bai, T.; Yan, H.; Ding, F.; Bai, L.; Feng, W. High Fluorescence Quantum Yield Based on the Through-Space Conjugation of Hyperbranched Polysiloxane. *Macromolecules* **2019**, *52* (8), 3075–3082. https://doi.org/10.1021/acs.macromol.9b00263.

(51) Tang, S.; Yang, T.; Zhao, Z.; Zhu, T.; Zhang, Q.; Hou, W.; Yuan, W. Z. Nonconventional Luminophores: Characteristics, Advancements and Perspectives. *Chem Soc Rev* **2021**, *50* (22), 12616–12655. https://doi.org/10.1039/d0cs01087a.